6

Time Discretization

In many practical applications the processes under consideration are unsteady and thus require for their numerical simulation the solution of time-dependent model equations. The time has a certain exceptional role in the differential equations because, unlike for spatial coordinates, there is a distinguished direction owing to the principle of causality. This fact has to be taken into account for the discretization techniques employed for time. In this chapter the most important aspects with respect to this issue are discussed.

6.1 Basics

For unsteady processes the physical quantities – in addition to the spatial dependence – also depend on the time t. In the applications considered here mainly two types of time-dependent problems appear: transport and vibration processes. Examples of corresponding processes are, for instance, the Kármán vortex street formed when fluids flow around bodies (see Fig. 6.1), or vibrations of a structure (see Fig. 6.2), respectively.

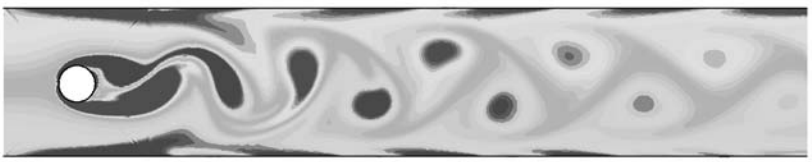

Fig. 6.1. Kármán vortex street (instantaneous vorticity)

While the equations for unsteady transport processes only involve first derivatives with respect to time, for vibration processes second time derivatives also appear. In the first case the problem is called *parabolic*, in the second case *hyperbolic*. Since we do not need the underlying concepts in the following,

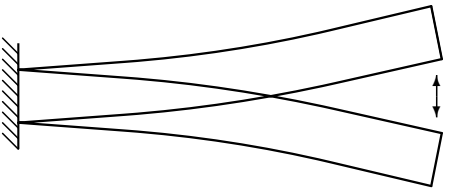

Fig. 6.2. Vibrations of a clamped beam

we will disperse with a more precise definition of the terms that can be used for a general classification of second-order partial differential equations (see, e.g., [9] or [12]).

An example of a parabolic problem is the general unsteady scalar transport equation (cf. Sect. 2.3.2)

$$\frac{\partial(\rho\phi)}{\partial t} + \frac{\partial}{\partial x_i}\left(\rho v_i \phi - \alpha \frac{\partial \phi}{\partial x_i}\right) = f\,. \tag{6.1}$$

An example of the hyperbolic type are the equations of linear elastodynamics (cf. Sect. 2.4.1). For a vibrating beam, as illustrated in Fig. 6.2, one has, for instance:

$$\rho A \frac{\partial^2 w}{\partial t^2} + \frac{\partial^2}{\partial x^2}\left(B \frac{\partial^2 w}{\partial x^2}\right) + f_{\mathrm{q}} = 0\,. \tag{6.2}$$

Compared to the corresponding steady problems the time is an additional coordinate, i.e., $\phi = \phi(\mathbf{x}, t)$ or $w = w(\mathbf{x}, t)$. Also, all involved prescribed quantities may depend on time. Note that vibration processes frequently can be formulated by means of a separation ansatz, i.e., $\phi(\mathbf{x}, t) := \phi_1(\mathbf{x})\,\phi_2(t)$, in the form of eigenvalue problems. However, we will not go into further detail with this here (see, e.g., [2]).

In order to fully define time-dependent problems, initial conditions are required in addition to the boundary conditions (which may also depend on time). For transport problems an initial distribution of the unknown function has to be prescribed, e.g.,

$$\phi(\mathbf{x}, t_0) = \phi^0(\mathbf{x})$$

for problem (6.1), while vibration problems require an additional initial distribution for the first time derivative, e.g.,

$$w(x, t_0) = w^0(x) \quad \text{und} \quad \frac{\partial w}{\partial t}(x, t_0) = w^1(x)$$

for problem (6.2).

For the numerical solution of time-dependent problems usually first a spatial discretization with one of the techniques described in the preceding sections is performed. This results in a system of ordinary differential equations (with respect to time). In a finite-difference method setting this approach is

referred to as *method of lines*. For instance, the spatial discretization of (6.1) with a finite-volume method yields for each control volume the equation

$$\frac{\partial \phi_\mathrm{P}}{\partial t} = \frac{1}{\rho\, \delta V} \left[-a_\mathrm{P}(t)\phi_\mathrm{P} + \sum_c a_c(t)\phi_c + b_\mathrm{P}(t) \right] , \tag{6.3}$$

where, for the sake of simplicity we assume the density ρ and the volume δV is temporally constant (and we will also do so in the following). Globally, i.e., for all control volumes, (6.3) corresponds to a (coupled) system of ordinary differential equations for the unknown functions $\phi_\mathrm{P}^i = \phi_\mathrm{P}^i(t)$ for $i = 1, \ldots, N$, where N is the number of control volumes.

When employing a finite-element method for the spatial discretization of a time-dependent problem, in the Galerkin method a corresponding ansatz with time-dependent coefficients is made:

$$\phi(\mathbf{x}, t) = \varphi_0(\mathbf{x}, t) + \sum_{k=1}^{N} c_k(t)\varphi_k(\mathbf{x}) .$$

For temporally varying boundary conditions also the function φ_0 has to be time-dependent, because it has to fulfil the inhomogeneous boundary conditions within the whole time interval. Applying the Galerkin method with this ansatz in an analogous way as in the steady case leads to a system of ordinary differential equations for the unknown functions $c_k = c_k(t)$ (see Exercise 6.2).

For ease of notation in the following the right hand side of the equation resulting from the spatial discretization (either obtained by finite-volume or finite-element methods) is expressed by the operator $\mathcal{L}$:

$$\frac{\partial \boldsymbol{\phi}}{\partial t} = \mathcal{L}(\boldsymbol{\phi}) ,$$

where $\boldsymbol{\phi} = \boldsymbol{\phi}(t)$ denotes the vector of the unknown functions. For instance, in the case of a finite-volume space discretization of (6.1) according to (6.3), the components of $\mathcal{L}(\boldsymbol{\phi})$ are defined by the right hand side of (6.3).

For the time discretization, i.e., for the discretization of the systems of ordinary differential equations, techniques similar to those for the spatial coordinates can be employed (i.e., finite-difference, finite-volume, or finite-element methods). Since the application of the different methods does not result in principal differences in the resulting discrete systems, we restrict ourselves to the (most simple) case of finite-difference approximations.

First, the time interval $[t_0, T]$ under consideration is divided into individual, generally non-equidistant, subintervals Δt_n:

$$t_{n+1} = t_n + \Delta t_n , \quad n = 0, 1, 2, \ldots$$

For a further simplification of notation the variable value at time t_n is indicated with an index n, e.g.:

$$\mathcal{L}(\boldsymbol{\phi}(t_n)) = \mathcal{L}(\boldsymbol{\phi}^n).$$

According to the principle of causality the solution at time t_{n+1} only can depend on *previous* points in time t_n, t_{n-1}, ... Since the time in this sense is a "one-way" coordinate, the solution for t_{n+1} has to be determined as a function of the boundary conditions and the solutions at earlier times. Thus, the time discretization always consists in an extrapolation. Starting from the prescribed initial conditions at t_0, the unknown variable ϕ is successively computed at the points of time t_1, t_2, ... (see Fig. 6.3).

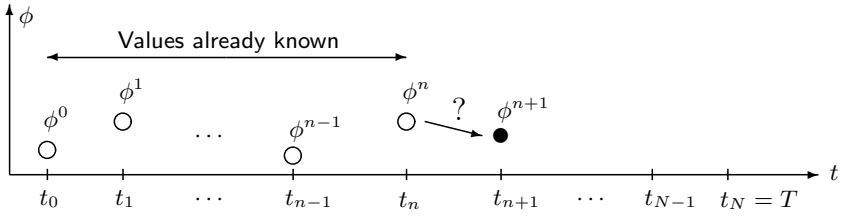

Fig. 6.3. Time-stepping process

Finally, the temporal developing of ϕ can be represented as a sequence of different spatial values at discrete points in time (see Fig. 6.4 for a spatially two-dimensional problem). It should be noted that for transport problems steady solutions are often also computed with a time discretization method as a limit for $t \to \infty$ from the time-dependent equations. However, this method, known as *pseudo time stepping*, does not usually result in an efficient method, but may be useful when, owing to stability problems, the direct solution of the steady problem is hard to obtain (the time-stepping acts as a relaxation, see Sect. 10.3.3).

There must be at least *one* already known time level to discretize the time derivative. If only one time level is used, i.e., the values at t_n, one speaks of *one-step methods*, while if more known time levels are employed, i.e., values for

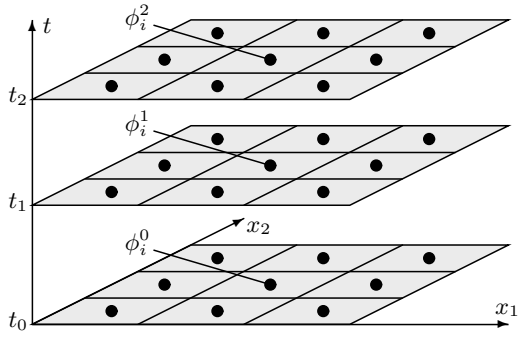

Fig. 6.4. Relation between spatial and temporal discretization

the time levels $t_n, t_{n-1}, \ldots$, one talks about *multi-step methods*. Furthermore – and more importantly – the methods for the time discretization generally are divided into two classes according to the choice of points of time, at which the right hand side is evaluated:

- *Explicit methods*: discretization of the right hand side only at previous (already known) time levels:

$$\boldsymbol{\phi}^{n+1} = \mathcal{F}(\boldsymbol{\phi}^n, \boldsymbol{\phi}^{n-1}, \ldots) \,.$$

- *Implicit methods*: discretization of the right hand side also at new (unknown) time level:

$$\boldsymbol{\phi}^{n+1} = \mathcal{F}(\boldsymbol{\phi}^{n+1}, \boldsymbol{\phi}^n, \boldsymbol{\phi}^{n-1}, \ldots) \,.$$

Here, $\mathcal{F}$ denotes some discretization rule for the choice of which we will give examples later. The distinction into explicit and implicit methods is a very important attribute because far reaching differences with respect to the properties of the numerical schemes arise (we will go into more detail in Sect. 8.1.2).

In the next two sections some important and representative variants for the above classes of methods will be introduced. We restrict our considerations to problems of the parabolic type (only first time derivative). However, it should be mentioned that the described methods in principle also can be applied to problems with second time derivative, i.e., problems of the type

$$\frac{\partial^2 \boldsymbol{\phi}}{\partial t^2} = \mathcal{L}(\boldsymbol{\phi}) \,, \tag{6.4}$$

by introducing the first time derivatives

$$\boldsymbol{\psi} = \frac{\partial \boldsymbol{\phi}}{\partial t}$$

as additional unknowns (order reduction). According to (6.4) one has

$$\frac{\partial \boldsymbol{\psi}}{\partial t} = \mathcal{L}(\boldsymbol{\phi})$$

and with the definitions

$$\tilde{\boldsymbol{\phi}} = \begin{bmatrix} \boldsymbol{\psi} \\ \boldsymbol{\phi} \end{bmatrix} \quad \text{and} \quad \tilde{\mathcal{L}}(\tilde{\boldsymbol{\phi}}) = \begin{bmatrix} \mathcal{L}(\boldsymbol{\phi}) \\ \boldsymbol{\psi} \end{bmatrix}$$

a system of the form

$$\frac{\partial \tilde{\boldsymbol{\phi}}}{\partial t} = \tilde{\mathcal{L}}(\tilde{\boldsymbol{\phi}})$$

results, which is equivalent to (6.4) and involves only first time derivatives. However, this way the number of unknowns doubles so that methods that solve the system (6.4) directly (for instance the so-called *Newmark methods*, see, e.g., [2]) usually are more efficient.

6.2 Explicit Methods

We start with the most simple example of a time discretization method, the *explicit Euler method*, which is obtained by approximating the time derivative at time level t_n by means of a forward differencing scheme:

$$\frac{\partial \boldsymbol{\phi}}{\partial t}(t_n) \approx \frac{\boldsymbol{\phi}^{n+1} - \boldsymbol{\phi}^n}{\Delta t_n} = \mathcal{L}(\boldsymbol{\phi}^n)\,. \tag{6.5}$$

This corresponds to an approximation of the time derivative of the components ϕ_i of $\boldsymbol{\phi}$ at the time t_n by means of the slope of the straight line through the points ϕ_i^n and ϕ_i^{n+1} (see Fig. 6.5). The method is first-order accurate (with respect to time) and is also known as the *Euler polygon method*.

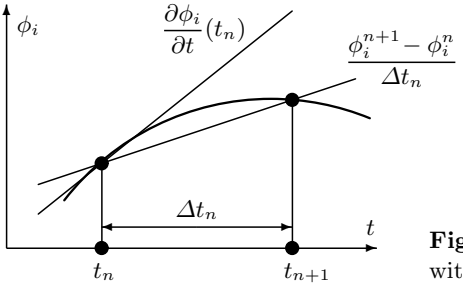

Fig. 6.5. Approximation of time derivative with explicit Euler method

The relation (6.5) can be resolved explicitly for $\boldsymbol{\phi}^{n+1}$:

$$\boldsymbol{\phi}^{n+1} = \boldsymbol{\phi}^n + \Delta t_n \mathcal{L}(\boldsymbol{\phi}^n)\,.$$

On the right hand side there are only values from the already known time level, such that the equations for the values at the point of time t_{n+1} at the different spatial grid points are fully decoupled and can be computed independently from each other. This is characteristic for explicit methods.

Let us consider as an example the unsteady one-dimensional diffusion equation (with constant material parameters):

$$\frac{\partial \phi}{\partial t} = \frac{\alpha}{\rho}\,\frac{\partial^2 \phi}{\partial x^2}\,. \tag{6.6}$$

A finite-volume space discretization with the central differencing scheme for the diffusion term for an equidistant grid with grid spacing Δx yields for each control volume the ordinary differential equation:

$$\frac{\partial \phi_\mathrm{P}}{\partial t}(t)\,\Delta x = \frac{\alpha}{\rho}\,\frac{\phi_\mathrm{E}(t) - \phi_\mathrm{P}(t)}{\Delta x} - \frac{\alpha}{\rho}\,\frac{\phi_\mathrm{P}(t) - \phi_\mathrm{W}(t)}{\Delta x} \tag{6.7}$$

The explicit Euler method with fixed time step size Δt gives the following approximation:

$$\frac{\phi_{\mathrm{P}}^{n+1} - \phi_{\mathrm{P}}^{n}}{\Delta t}\,\Delta x = \frac{\alpha}{\rho}\,\frac{\phi_{\mathrm{E}}^{n} - \phi_{\mathrm{P}}^{n}}{\Delta x} - \frac{\alpha}{\rho}\,\frac{\phi_{\mathrm{P}}^{n} - \phi_{\mathrm{W}}^{n}}{\Delta x}$$

Resolving for ϕ_{P}^{n+1} yields

$$\phi_{\mathrm{P}}^{n+1} = \frac{\alpha \Delta t}{\rho \Delta x^2}(\phi_{\mathrm{E}}^{n} + \phi_{\mathrm{W}}^{n}) + (1 - \frac{2\alpha \Delta t}{\rho \Delta x^2})\phi_{\mathrm{P}}^{n}\,.$$

The procedure is illustrated graphically in Fig. 6.6. One observes that a number of time steps is necessary until changes at the boundary affect the interior of the spatial problem domain. The finer the grid, the slower the spreading of the information (for the same time step size). As we will see in Sect. 8.1.2, this leads to a limitation of the time step size (stability condition), which depends quadratically on the spatial resolution and, with a finer spatial grid, becomes more and more restrictive. This limitation is purely due to numerical reasons and independent from the actual temporal developing of the problem solution.

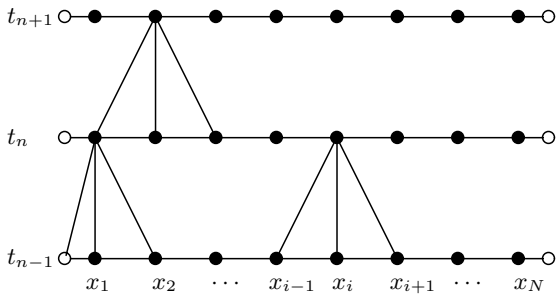

Fig. 6.6. Procedure and flow of information for explicit Euler method

There are numerous other explicit one-step methods that differ from the explicit Euler method in the approximation of the right hand sides. The *modified explicit Euler method* formulated by Collatz (1960) is

$$\frac{\boldsymbol{\phi}^{n+1} - \boldsymbol{\phi}^{n}}{\Delta t_n} = \mathcal{L}(\boldsymbol{\phi}^{n} + \frac{\Delta t_n}{2}\mathcal{L}(\boldsymbol{\phi}^{n}))\,,$$

which, compared to the explicit Euler method, requires just one additional evaluation of the right hand side, but is second order accurate on equidistant grids.

Another class of explicit one-step methods are the *Runge-Kutta methods*, which are frequently used in practice particularly for aerodynamical flow simulations. These methods can be defined for arbitrary order. As an example, the classical Runge-Kutta method of fourth order is defined by:

$$\frac{\boldsymbol{\phi}^{n+1} - \boldsymbol{\phi}^{n}}{\Delta t_n} = \frac{1}{6}(f_1 + 2f_2 + 2f_3 + f_4)\,,$$

where

$$f_1 = \mathcal{L}(\boldsymbol{\phi}^n)\,, \qquad f_2 = \mathcal{L}(\boldsymbol{\phi}^n + \frac{\Delta t_n}{2} f_1)\,,$$
$$f_3 = \mathcal{L}(\boldsymbol{\phi}^n + \frac{\Delta t_n}{2} f_2)\,, \quad f_4 = \mathcal{L}(\boldsymbol{\phi}^n + \Delta t_n f_3)\,.$$

Combinations of Runge-Kutta methods of the orders p and $p+1$ frequently are employed to obtain procedures with an automatic time step size control. The resulting methods are known as *Runge-Kutta-Fehlberg methods* (see, e.g., [24]).

In multi-step methods more than two time levels are employed to approximate the time derivative. A corresponding discretization scheme can, for instance, be defined by assuming a piecewise polynomial course of the unknown function with respect to time (e.g., quadratically for three time levels) or by a suitable Taylor series expansion (see, e.g., [12]).

The computation of the solution with a multi-step method must always be started with a single-step method because initially only the solution at t_0 is available. Having computed the solutions for $t_1, \ldots, t_{p-2}$, one can continue with a p time level method. Note that during the computation all variable values from the involved time levels have to be stored. In the case of large systems and many time levels this results in a relatively large memory requirement.

Depending on the number of involved time levels, the approximation of the time derivative, and the evaluation of the right hand side, a variety of multi-step methods can be defined. An important class of explicit multi-step methods that are frequently employed in practice are the *Adams-Bashforth methods*. These can be derived by polynomial interpolation with arbitrary orders. However, in practice, only the methods up to the order 4 are used. For equdistant time steps these are summarized in Table 6.1 (the first order Adams-Bashforth method is again the explicit Euler method).

Table 6.1. Adams-Bashforth methods up to the order 4

Formula	Order
$\frac{\boldsymbol{\phi}^{n+1} - \boldsymbol{\phi}^n}{\Delta t} = \mathcal{L}(\boldsymbol{\phi}^n)$	1
$\frac{\boldsymbol{\phi}^{n+1} - \boldsymbol{\phi}^n}{\Delta t} = \frac{1}{2}\left[3\mathcal{L}(\boldsymbol{\phi}^n) - \mathcal{L}(\boldsymbol{\phi}^{n-1})\right]$	2
$\frac{\boldsymbol{\phi}^{n+1} - \boldsymbol{\phi}^n}{\Delta t} = \frac{1}{12}\left[23\mathcal{L}(\boldsymbol{\phi}^n) - 16\mathcal{L}(\boldsymbol{\phi}^{n-1}) + 5\mathcal{L}(\boldsymbol{\phi}^{n-2})\right]$	3
$\frac{\boldsymbol{\phi}^{n+1} - \boldsymbol{\phi}^n}{\Delta t} = \frac{1}{24}\left[55\mathcal{L}(\boldsymbol{\phi}^n) - 59\mathcal{L}(\boldsymbol{\phi}^{n-1}) + 37\mathcal{L}(\boldsymbol{\phi}^{n-2}) - 9\mathcal{L}(\boldsymbol{\phi}^{n-3})\right]$	4

6.3 Implicit Methods

Approximating the time derivative at time t_{n+1} by a first order backward difference formula (see Fig. 6.7) results in the *implicit Euler method*:

$$\frac{\partial \boldsymbol{\phi}}{\partial t}(t_{n+1}) \approx \frac{\boldsymbol{\phi}^{n+1} - \boldsymbol{\phi}^{n}}{\Delta t_n} = \mathcal{L}(\boldsymbol{\phi}^{n+1})$$

This differs from the explicit variant only in the evaluation of the right hand side, which now is computed at the new (unknown) time level. Consequently, explicitly solving for ϕ_{P}^{n+1} is no longer possible because all variables of the new time level are coupled to each other. Thus, for the computation of *each* new time level – as in the steady case – the solution of an equation system is necessary. This is characteristic for implicit methods.

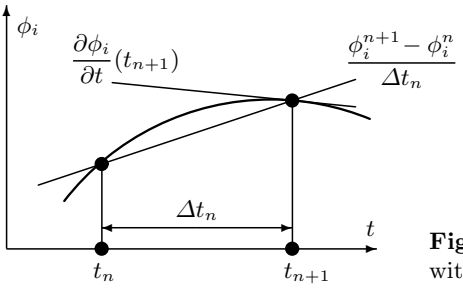

Fig. 6.7. Approximation of time derivative with implicit Euler method

For instance, discretizing the one-dimensional diffusion equation (6.6) with the spatial discretization (6.7) using the implicit Euler method gives:

$$(1 + \frac{2\alpha \Delta t}{\rho \Delta x^2})\phi_{\mathrm{P}}^{n+1} = \frac{\alpha \Delta t}{\rho \Delta x^2}(\phi_{\mathrm{E}}^{n+1} + \phi_{\mathrm{W}}^{n+1}) + \phi_{\mathrm{P}}^{n}\,. \tag{6.8}$$

Regarded over all control volumes, this represents a tridiagonal linear equation system that has to be solved for each time step.

In the implicit case changes at the boundary in the actual time step spread in the whole spatial problem domain (see Fig. 6.8) so that the stability problems indicated for the explicit Euler method do not occur in this form. The implicit Euler method turns out to be stable independently of Δx and Δt (see Sect. 8.1.2).

As the explicit method, the implicit Euler method is first order accurate in time. It is more costly than the explicit variant because more computational effort (for the solution the equation system) and more memory (for the coefficients and the source terms) is required per time step. However, there is no limitation for the time step size due to stability reasons. The higher effort of the method usually is more than compensated for by the possibility of selecting larger time steps. Thus, in most cases it is in total much more efficient than the explicit variant.

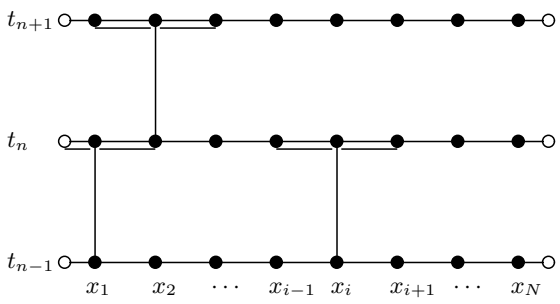

Fig. 6.8. Procedure and flow of information for implicit Euler method

The algebraic equations resulting with the implicit Euler method for an unsteady transport problem differ from the corresponding steady case (when using the same spatial discretizations) only by two additional terms in the coefficients a_P and b_P:

$$\underbrace{(a_\mathrm{P}^{n+1} + \boxed{\frac{\delta V \rho}{\Delta t_n}})}_{\tilde{a}_\mathrm{P}^{n+1}} \phi_\mathrm{P}^{n+1} = \sum_c a_c^{n+1} \phi_c^{n+1} + \underbrace{b_\mathrm{P}^{n+1} + \boxed{\frac{\delta V \rho}{\Delta t_n} \phi_\mathrm{P}^n}}_{\tilde{b}_\mathrm{P}^{n+1}}.$$

In the limit $\Delta t_n \to \infty$ the steady equations result. Thus, the methods can be easily combined for a single code that can handle both steady and unsteady cases.

An important implicit one-step method frequently used in practice is the *Crank-Nicolson method*, which is obtained when for each component ϕ_i of $\boldsymbol{\phi}$ the time derivative at time $t_{n+1/2} = (t_n + t_{n+1})/2$ is approximated by the straight line connecting ϕ_i^{n+1} and ϕ_i^n (see Fig. 6.9):

$$\frac{\partial \boldsymbol{\phi}}{\partial t}(t_{n+1/2}) \approx \frac{\boldsymbol{\phi}^{n+1} - \boldsymbol{\phi}^n}{\Delta t_n} = \frac{1}{2} \left[\mathcal{L}(\boldsymbol{\phi}^{n+1}) + \mathcal{L}(\boldsymbol{\phi}^n) \right] .$$

This corresponds to a central difference approximation of the time derivative at time $t_{n+1/2}$. The scheme has a second order temporal accuracy. The method is also called trapezoidal rule because the application of the latter for numerical integration of the equivalent integral equation yields the same formula.

The computational effort for the Crank-Nicolson method is only slightly higher than for the implicit Euler method because only $\mathcal{L}(\boldsymbol{\phi}^n)$ has to be computed additionally and the solution of the resulting equation systems usually is a bit more "difficult". However, due to the higher order the accuracy is much better. One can show that the Crank-Nicolson method is the most accurate second-order method.

For problem (6.6) with the spatial discretization (6.7), the Crank-Nicolson method results in the following approximation:

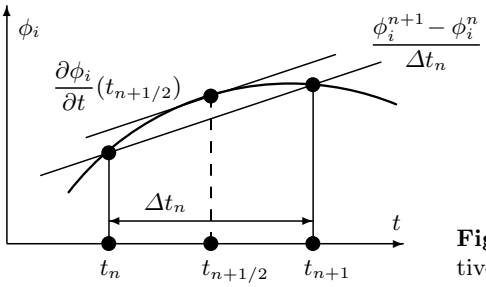

Fig. 6.9. Approximation of time derivative with Crank-Nicolson method

$$2(1 + \frac{\alpha \Delta t}{\rho \Delta x^2})\phi_{\mathrm{P}}^{n+1} = \frac{\alpha \Delta t}{\rho \Delta x^2}(\phi_{\mathrm{E}}^{n+1} + \phi_{\mathrm{W}}^{n+1}) + \frac{\alpha \Delta t}{\rho \Delta x^2}(\phi_{\mathrm{E}}^{n} + \phi_{\mathrm{W}}^{n}) + 2(1 - \frac{\alpha \Delta t}{\rho \Delta x^2})\phi_{\mathrm{P}}^{n} .$$

Although it is implicit, the Crank-Nicolson method may suffer from stability problems for cases where the problem solution is spatially not "smooth" (no *strong A-stability*, see, e.g., [12]). By interspersing some steps of the implicit Euler method at regular intervals, a damping of the corresponding (non-physical) oscillations can be achieved while preserving the second-order accuracy of the scheme.

Note that the explicit and implicit Euler methods as well as the Crank-Nicolson method can be integrated into a single code in a simple way by introducing a control parameter θ as follows:

$$\frac{\boldsymbol{\phi}^{n+1} - \boldsymbol{\phi}^n}{\Delta t_n} = \theta \mathcal{L}(\boldsymbol{\phi}^{n+1}) + (1 - \theta)\mathcal{L}(\boldsymbol{\phi}^n) .$$

This approach in the literature is often called *θ-method*. For $\theta = 0$ and $\theta = 1$ the explicit and implicit Euler methods, respectively, result. $\theta = 1/2$ gives the Crank-Nicolson method. Valid time discretizations are also obtained for all other values of θ in the interval $[0, 1]$. However, for $\theta \neq 1/2$ the method is only of first order.

As in the explicit case, implicit multi-step methods of different order can be defined depending on the number of involved time levels, the approximation of the time derivative, and the evaluation of the right hand side An important class of methods are the *BDF-methods* (backward-differencing formula). These can be derived with arbitrary order by approximating the time derivative at t_{n+1} with backward-differencing formulas involving a corresponding number of previous time levels. The corresponding methods for equidistant time steps up to the order 4 are indicated in Table 6.2.

The first order BDF-method corresponds to the implicit Euler method. In particular, the second order BDF-method is frequently used in practice. With this the unknown function is approximated by the parabola defined by the function values at the time levels t_{n-1}, t_n, and t_{n+1} (see Fig. 6.10). Having comparably good stability properties this method only involves slightly

Table 6.2. BDF-methods up to the order 4

Formula	Order
$\frac{\boldsymbol{\phi}^{n+1}-\boldsymbol{\phi}^{n}}{\Delta t}=\mathcal{L}(\boldsymbol{\phi}^{n+1})$	1
$\frac{3\boldsymbol{\phi}^{n+1}-4\boldsymbol{\phi}^{n}+\boldsymbol{\phi}^{n-1}}{2\Delta t}=\mathcal{L}(\boldsymbol{\phi}^{n+1})$	2
$\frac{11\boldsymbol{\phi}^{n+1}-18\boldsymbol{\phi}^{n}+9\boldsymbol{\phi}^{n-1}+2\boldsymbol{\phi}^{n-2}}{6\Delta t}=\mathcal{L}(\boldsymbol{\phi}^{n+1})$	3
$\frac{25\boldsymbol{\phi}^{n+1}-48\boldsymbol{\phi}^{n}+36\boldsymbol{\phi}^{n-1}-16\boldsymbol{\phi}^{n-2}+3\boldsymbol{\phi}^{n-3}}{2\Delta t}=\mathcal{L}(\boldsymbol{\phi}^{n+1})$	4

more computational effort per time step and is much more accurate than the implicit Euler method. Only the values $\boldsymbol{\phi}^{n-1}$ have to be stored additionally. From order three on the stability properties deteriorate with increasing order such that the application of a BDF-method with order higher than 4 is not recommended.

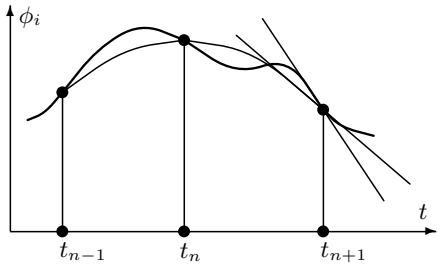

Fig. 6.10. Approximation of time derivative with second-order BDF-method

Another class of implicit multi-step methods are the *Adams-Moulton methods* – the implicit counterparts to the (explicit) Adams-Bashforth methods. The corresponding formulas up to the order 4 for equidistant grids are summarized in Table 6.3. The Adams-Moulton methods of first and second orders correspond to the implicit Euler and Crank-Nicolson methods, respectively.

Adams-Moulton methods can be used together with Adams-Bashforth methods of the same order as *predictor-corrector methods*. Here, the idea is to determine with the explicit predictor method in a "cheap" way a good starting value for the implicit corrector method. For instance, the corresponding predictor-corrector method of fourth order is given by:

$$\boldsymbol{\phi}^{*}=\boldsymbol{\phi}^{n}+\frac{\Delta t}{24}\left[55\mathcal{L}(\boldsymbol{\phi}^{n})-59\mathcal{L}(\boldsymbol{\phi}^{n-1})+37\mathcal{L}(\boldsymbol{\phi}^{n-2})-9\mathcal{L}(\boldsymbol{\phi}^{n-3})\right],$$
$$\boldsymbol{\phi}^{n+1}=\boldsymbol{\phi}^{n}+\frac{\Delta t}{24}\left[9\mathcal{L}(\boldsymbol{\phi}^{*})+19\mathcal{L}(\boldsymbol{\phi}^{n})-5\mathcal{L}(\boldsymbol{\phi}^{n-1})+\mathcal{L}(\boldsymbol{\phi}^{n-2})\right].$$

Table 6.3. Adams-Moulton methods up to the order 4

Formula	Order
$\frac{\boldsymbol{\phi}^{n+1}-\boldsymbol{\phi}^n}{\Delta t} = \mathcal{L}(\boldsymbol{\phi}^{n+1})$	1
$\frac{\boldsymbol{\phi}^{n+1}-\boldsymbol{\phi}^n}{\Delta t} = \frac{1}{2}\left[\mathcal{L}(\boldsymbol{\phi}^{n+1}) + \mathcal{L}(\boldsymbol{\phi}^n)\right]$	2
$\frac{\boldsymbol{\phi}^{n+1}-\boldsymbol{\phi}^n}{\Delta t} = \frac{1}{12}\left[5\mathcal{L}(\boldsymbol{\phi}^{n+1}) + 8\mathcal{L}(\boldsymbol{\phi}^n) - \mathcal{L}(\boldsymbol{\phi}^{n-1})\right]$	3
$\frac{\boldsymbol{\phi}^{n+1}-\boldsymbol{\phi}^n}{\Delta t} = \frac{1}{24}\left[9\mathcal{L}(\boldsymbol{\phi}^{n+1}) + 19\mathcal{L}(\boldsymbol{\phi}^n) - 5\mathcal{L}(\boldsymbol{\phi}^{n-1}) + \mathcal{L}(\boldsymbol{\phi}^{n-2})\right]$	4

The error for such a combined method is equal to that of the implicit method, which is always the smaller one.

6.4 Numerical Example

As a more complex application example for the numerical simulation of time-dependent processes and for comparison of different time discretization methods we consider the unsteady flow around a circular cylinder in a channel with time dependent inflow condition. The problem configuration is shown in Fig. 6.11. The problem can be described by the two-dimensional incompressible Navier-Stokes equations as given in Sect. 2.5.1. The kinematic viscosity is defined as $\nu = 10^{-3}\,\mathrm{m}^2/\mathrm{s}$, and the fluid density is $\rho = 1.0\,\mathrm{kg/m}^3$. The inflow condition for the velocity component v_1 in x_1-direction is

$$v_1(0, x_2, t) = 4v_{\max} x_2 (H - x_2)\sin(\pi t/8)/H^2\,, \quad \text{for} \quad 0 \le t \le 8\,\mathrm{s}$$

with $v_{\max} = 1.5\,\mathrm{m/s}$. This corresponds to the velocity profile of a fully developed channel flow, where the Reynolds number $Re = \bar{v}D/\nu$ based on the cylinder diameter $D = 0.1\,\mathrm{m}$ and the mean velocity $\bar{v}(t) = 2v_{\max}(0, H/2, t)/3$ varies in the range $0 \le \mathrm{Re} \le 100$.

As reference quantities the drag and lift coefficients

$$c_\mathrm{D} = \frac{2F_w}{\rho \bar{v}^2 D} \quad \text{and} \quad c_\mathrm{L} = \frac{2F_a}{\rho \bar{v}^2 D}$$

for the cylinder are considered. Hereby, the drag and lift forces are defined by

$$F_\mathrm{D} = \int_S (\rho\nu \frac{\partial v_t}{\partial x_i} n_i n_2 - p n_1)\,\mathrm{d}S \quad \text{and} \quad F_\mathrm{L} = -\int_S (\rho\nu \frac{\partial v_t}{\partial x_i} n_i n_1 + p n_2)\,\mathrm{d}S\,,$$

where S denotes the cylinder surface (circle), $\mathbf{n} = (n_1, n_2)$ is the normal vector on S, and v_t is the tangential velocity on S.

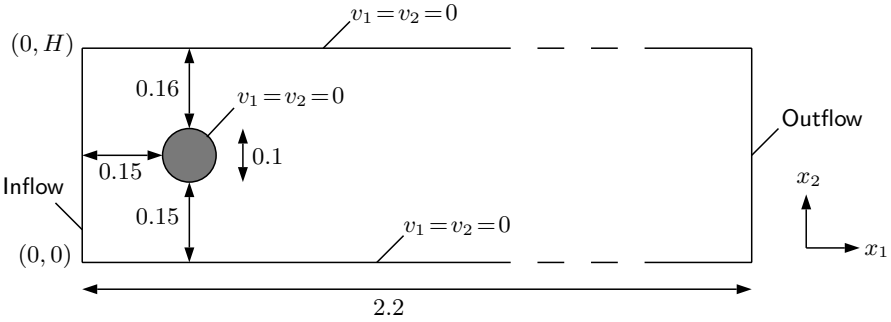

Fig. 6.11. Configuration for two-dimensional flow around cylinder (lengths in m)

The temporal development of the flow is illustrated in Fig. 6.12 and shows the vorticity at different points of time. First, there are two counterrotating vortices behind the cylinder, that become unstable after a certain time (with increasing oncoming flow). A Kármán vortex street forms and finally decays with decreasing oncoming flow. The problem effectively involves two kinds of time dependencies: an "outer" one due to the time-dependent boundary condition and an "inner" one due to the vortex separation by physical instability (bifurcation).

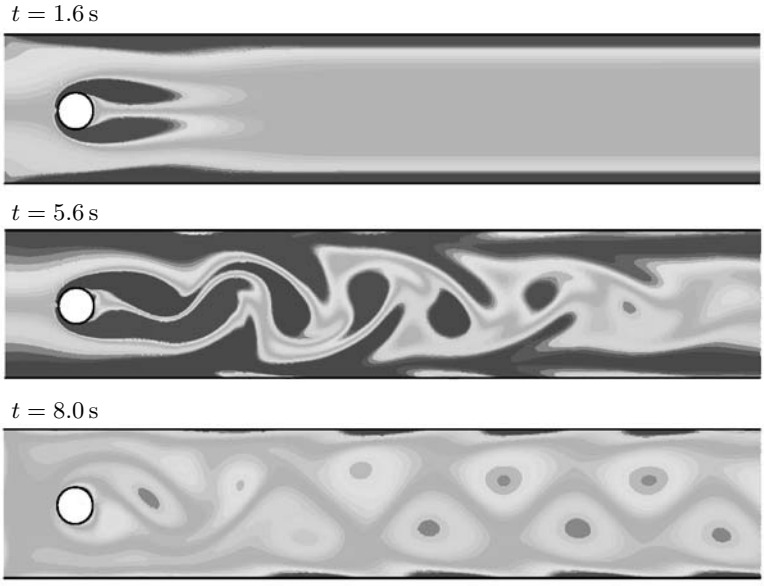

Fig. 6.12. Temporal development of vorticity for unsteady flow around cylinder

The spatial discretization uses a finite-volume method with central differencing scheme on a grid with 24 576 CVs, a typical grid size for this kind of problem. The grid can be seen in Fig. 6.13, where for visibility only every fourth grid line is shown, i.e., the real number of CVs is 16 times larger. For the time discretization the implicit Euler method, the Crank-Nicolson method, and the second-order BDF-method are compared. We only consider implicit methods because explicit methods for this kind of problems are orders of magnitude slower and, therefore, are out of discussion here.

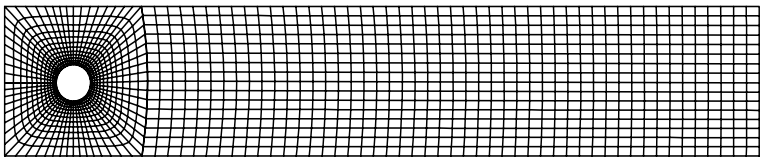

Fig. 6.13. Numerical grid for flow around cylinder (every fourth grid line is shown)

Figure 6.14 shows the temporal development of the lift coefficient c_{L} obtained with the different time discretization methods, where for each case the same time step size $\Delta t = 0.02\,\mathrm{s}$ is employed. Thus 400 time steps for the given time interval of 8 s are necessary. The "exact" solution, which has been obtained by a computation with a very fine grid and a very small time step size, is also indicated.

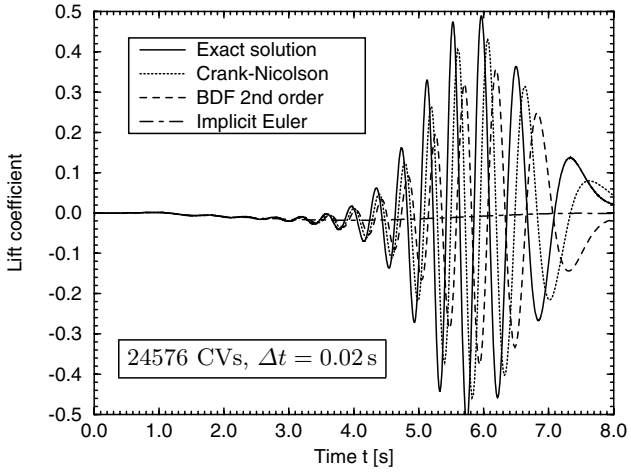

Fig. 6.14. Temporal development of lift coefficient for different time discretization schemes for flow around cylinder

One can see quite significant differences in the results obtained with the different methods. With the implicit Euler method the oscillations with the given time step size are not captured at all. The discretization error in this case is so large, that the oscillations are damped completely. The BDF-method is able to resolve the oscillations to some extent, but the amplitude is clearly too small. The Crank-Nicolson method, as one would expect from a corresponding analysis of the discretization error, gives the best result.

One of the most important practical aspects for a numerical method is how much computing time the method needs to compute the solution with a certain accuracy. In order to compare the methods in this respect, Fig. 6.15 shows the relative error for the maximum of the lift coefficient against the computing time, which is needed for different time step sizes, for the different time discretization methods.

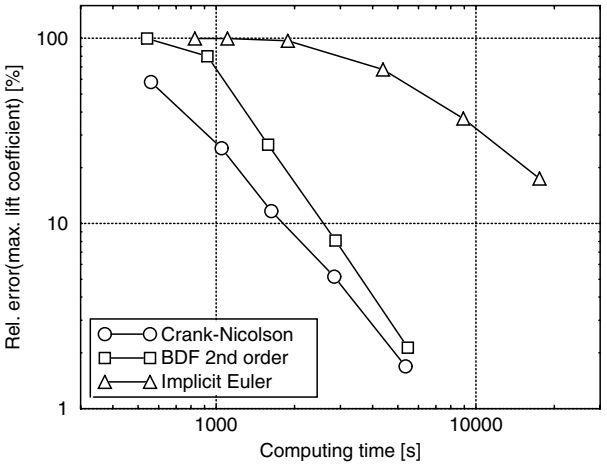

Fig. 6.15. Relative error against computing time for different time discretizations

One can observe that the implicit Euler method does not perform well because very small time step sizes are necessary to achieve an acceptable accuracy (the method is only of first order). The two second-order methods don't differ that much, in particular, in the range of small errors. However, the Crank-Nicolson method is also in this respect the best scheme, i.e., within a given computing time with this method one obtains the most accurate results. In other words, a precribed accuracy can be achieved within the shortest computing time.

In order to point out that not all quantities of a problem react with the same sensitivity to the discretization employed, in Fig. 6.16 the temporal development of the drag coefficient c_{D} that results with the different time

discretization schemes is given. In contrast to the corresponding lift coefficients one can observe only minor differences in the results for the different methods.

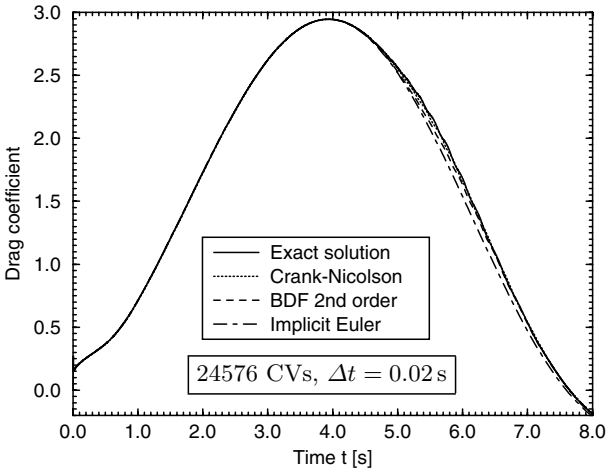

Fig. 6.16. Temporal development of drag coefficient with different time discretizations

In summary, one can conclude that the time discretization method together with the time step size has to be chosen according to the accuracy requirements of the underlying problem, where the stability and approximation properties of the method have to be taken into account. This is not always an easy undertaking. In the case of strong temporal variations in the solution, the method should in any event be at least of second order.

Exercises for Chap. 6

Exercise 6.1. The temperature distribtion $T = T(t, x)$ in a bar of length L with constant material properties is decribed by the differential equation

$$\frac{\partial T}{\partial t} - \alpha \frac{\partial^2 T}{\partial x^2} = 0 \quad \text{with} \quad \alpha = \frac{\kappa}{\rho c_p}$$

for $0 < x < L$ and $t > 0$ (cf. Sect. 2.3.2). As initial and boundary conditions $T(0, x) = \sin(\pi x) + x$ and $T(t, 0) = 0$, and $T(t, L) = 1$ are given (in K). The problem parameters are $L = 1\,\mathrm{m}$ and $\alpha = 1\,\mathrm{m}^2/\mathrm{s}$. (i) Use the FVM with two equidistant CVs and second-order central differences for the spatial discretization and formulate the resulting ordinary differential equations for the two CVs. (ii) Compute the temperature until the time $t = 0,4\,\mathrm{s}$ with the implicit and explicit Euler methods, each with $\Delta t = 0,1\,\mathrm{s}$ and $0,2\,\mathrm{s}$. (iii) Discuss the

results in comparison to the analytic solution $T_\mathrm{a}(t,x) = e^{-\alpha t \pi^2} \sin(\pi x) + x$.

Exercise 6.2. Discretize the unsteady transport equation (2.24) with the finite-element method and formulate the θ-method for the resulting system of ordinary differential equations.

Exercise 6.3. Formulate the Adams-Bashforth and the Adams-Moulton methods of fourth order for the problem in Exercise 6.1 and determine the corresponding truncation errors by Taylor series expansion.

Exercise 6.4. Formulate a second-order finite-volume method (for equidistant grids) for the spatial and temporal discretization of the unsteady beam equation (6.2).

Exercise 6.5. A finite-volume space discretization yields for $t > 0$ the system of ordinary differential equations

$$\begin{bmatrix} \phi_1' \\ \phi_2' \end{bmatrix} = \begin{bmatrix} 2 & 0 \\ t & \sqrt{t} \end{bmatrix} \begin{bmatrix} \phi_1 \\ \phi_2 \end{bmatrix} + \begin{bmatrix} \sin(\pi t) \\ \sqrt{t} \end{bmatrix}$$

for the two values $\phi_1 = \phi_1(t)$ and $\phi_2 = \phi_2(t)$ in the CV centers. The initial conditions are $\phi_1(0) = 2$ and $\phi_2(0) = 1$. (i) Discretize the system with the θ-method. (ii) Compute $\phi_1^1 = \phi_2(\Delta t)$ with the time step size $\Delta t = 2$.